scientific reports

Check for updates

OPEN

NKCC-1 mediated Cl^- uptake in immature CA3 pyramidal neurons is sufficient to compensate phasic GABAergic inputs

Sergey N. Kolbaev[1,5], Namrata Mohapatra[2], Rongqing Chen[1,6], Aniello Lombardi[1], Jochen F. Staiger[3], Heiko J. Luhmann[1], Peter Jedlicka[2,4] & Werner Kilb[1]✉

Activation of $GABA_A$ receptors causes in immature neurons a functionally relevant decrease in the intracellular Cl^- concentration ($[Cl^-]_i$), a process termed ionic plasticity. Amount and duration of ionic plasticity depends on kinetic properties of $[Cl^-]_i$ homeostasis. In order to characterize the capacity of Cl^- accumulation and to quantify the effect of persistent GABAergic activity on $[Cl^-]_i$, we performed gramicidin-perforated patch-clamp recordings from CA3 pyramidal neurons of immature (postnatal day 4–7) rat hippocampal slices. These experiments revealed that inhibition of NKCC1 decreased $[Cl^-]_i$ toward passive distribution with a time constant of 381 s. In contrast, active Cl^- accumulation occurred with a time constant of 155 s, corresponding to a rate of 15.4 µM/s. Inhibition of phasic GABAergic activity had no significant effect on steady state $[Cl^-]_i$. Inhibition of tonic GABAergic currents induced a significant $[Cl^-]_i$ increase by 1.6 mM, while activation of tonic extrasynaptic $GABA_A$ receptors with THIP significantly reduced $[Cl^-]_i$. Simulations of neuronal $[Cl^-]_i$ homeostasis supported the observation, that basal levels of synaptic GABAergic activation do not affect $[Cl^-]_i$. In summary, these results indicate that active Cl^--uptake in immature hippocampal neurons is sufficient to maintain stable $[Cl^-]_i$ at basal levels of phasic and to some extent also to compensate tonic GABAergic activity.

GABA (γ-amino butyric acid) is a major inhibitory neurotransmitter in the central nervous system of mammals[1] and is involved in the regulation of excitation, control of motor output or sensory integration, generation of oscillatory activity, neuronal assembly formation, and neuronal plasticity[2]. The responses to GABA are mediated via metabotropic $GABA_B$ receptors and ionotropic $GABA_A$ and $GABA_C$ receptors. $GABA_{A/C}$ receptors represent ligand-gated anion-channels with a high permeability for Cl^- ions, while HCO_3^- ions contribute only partially to the ionic currents[1]. During early neuronal development $GABA_A$ receptor-mediated responses are depolarizing, due to a high $[Cl^-]_i$[3]. This high $[Cl^-]_i$ is maintained by the activity of the isoform 1 of the Na^+-dependent K^+, Cl^- Cotransporter (NKCC1), which mediates an uptake of Cl^-[4–8]. The depolarizing GABAergic responses in the immature hippocampus have been associated with the generation of spontaneous oscillatory activity transients that are essential for brain development[9,10], but also to the higher incidence and pharmacological refractoriness of epileptic seizures in the immature CNS[11–14].

A variety of studies have demonstrated that the Cl^--fluxes through $GABA_A$ receptors influence $[Cl^-]_i$ on a shorter time scale and thus temporarily affect the amplitude of subsequent GABAergic responses[15–19]. This process is termed ionic plasticity[5,20]. Such activity-dependent $[Cl^-]_i$ transients have been implicated in a variety of pathophysiological processes[21–23], but they also underlie physiological functions, e.g. in the developing spinal cord where transient activity-dependent collapses of the Cl^- gradient generate slow oscillatory activity[7,24]. The size of activity-dependent Cl^- transients is on the first instance determined by the relation between Cl^- influx and the capacity of Cl^- extrusion systems[5,25]. Several computational studies revealed that, in addition to a variety

[1]Institute of Physiology, University Medical Center Mainz, Johannes Gutenberg University, Duesbergweg 6, 55128 Mainz, Germany. [2]Institute of Clinical Neuroanatomy, Neuroscience Center, Goethe-University, Theodor-Stern-Kai 7, 60590 Frankfurt, Germany. [3]Institute of Neuroanatomy, Universitätsmedizin Göttingen, Georg-August-Universität Göttingen, Kreuzbergring 36, 37075 Göttingen, Germany. [4]ICAR3R-Interdisciplinary Centre for 3Rs in Animal Research, Faculty of Medicine, Justus-Liebig-University, Rudolf-Buchheim-Str. 6, 35392 Giessen, Germany. [5]Present address: Research Center of Neurology, Volokolamskoyeshosse, 80, Moscow, Russia 125367. [6]Present address: Department of Neurobiology, School of Basic Medical Sciences, Southern Medical University, Guangzhou 510515, China. ✉email: wkilb@uni-mainz.de

of morphological and/or electrophysiological properties[26–28], the capacity of the transmembrane Cl^--transport is the main factor determining the spatiotemporal dynamics as well as the final amount of activity-dependent alterations in $[Cl^-]_i$[23,26,27,29–31]. Therefore, a quantification of the transport capacity of Cl^--extrusion or -uptake is necessary for a better understanding of GABAergic and glycinergic function during early development.

However, to our knowledge a detailed investigation of the kinetic properties of Cl^--transport has only been published for Cajal-Retzius cells[4] and immature spinal-cord motoneurons[7] as well as for mature cultured hippocampal[23] and thalamic neurons[32]. Whereas in mature hippocampal neurons the $[Cl^-]_i$ relaxation upon a massive $[Cl^-]_i$ increase occurs rather fast within ~ 30s[23], in immature neurons a rather inefficient Cl^--transport was observed[4,7]. In these neurons the recovery after $[Cl^-]_i$ depletion requires ~ 10–20 min[4,7]. Accordingly, it has been shown for both, Cajal-Retzius cells and immature motoneurons, that physiological levels of neuronal activity can cause functionally relevant changes in $[Cl^-]_i$[19,33]. Another striking example for activity-dependent changes in $[Cl^-]_i$ has been described in the immature hippocampus, where the massive GABAergic synaptic drive during giant depolarizing potentials, a network phenomenon essential for the development of hippocampal connectivity[34], causes massive alterations in $[Cl^-]_i$[17]. However, while several studies have already reported that the high $[Cl^-]_i$ of immature hippocampal neurons is maintained by NKCC1[14,35,36], to our knowledge no information about the kinetic properties of Cl^--transport in immature hippocampal neurons is available yet.

Therefore, we performed gramicidin-perforated patch-clamp recordings from visually identified CA3 pyramidal neurons of immature (postnatal day [P] 4–7) rat hippocampus to quantify the active and passive transport rates for Cl^- in immature hippocampal neurons. In addition, we analyzed whether baseline levels of synaptic and extrasynaptic GABAergic activity can influence $[Cl^-]_i$. Since the massive $[Cl^-]_i$ transients caused by GDPs would impair the analysis of the kinetic properties of $[Cl^-]_i$ homeostasis, we performed these experiments in coronal hippocampal slices, as in these slices only a fraction of connectivity is maintained[37] and therefore they fail to generate GDPs. Our experiments revealed that the rate of transmembrane Cl^--transport is rather low in immature CA3 neurons. Nevertheless, these transport rates are sufficient to maintain a stable $[Cl^-]_i$ during baseline synaptic GABAergic activity, while the physiological levels of tonic GABAergic currents provoke a slight shift in $[Cl^-]_i$.

Results

Steady-state distribution of $[Cl^-]_i$ in immature CA3 pyramidal cells. In this study we recorded in total from 121 CA3 pyramidal cells under gramicidin-perforated patch-clamp conditions. We estimated the reversal potential of GABAergic (E_{GABA}) and glycinergic (E_{Gly}) currents from short (2–10 ms) puffs of 30 µM muscimol or 0.2–1 mM glycine applied focally to the soma of the pyramidal cells (Fig. 1A). The use of glycine pulses was necessary for the determination of $[Cl^-]_i$ in part of the following experiments, as in these experiments gabazine or picrotoxin were used to eliminate phasic and tonic GABAergic currents. At a holding potential of − 70 mV these cells showed an E_{GABA} of − 57 [-55.6, -60.0] mV (n = 7) or an E_{Gly} of − 52 [-44.6, -62.7] mV (n = 58, Fig. 1B). Both values were not significantly different ($p = 0.315$, Mann–Whitney). Using published values for the HCO_3^- permeability of GABA (0.18) or glycine (0.11) receptors[38] and the estimated extra- and intracellular HCO_3^- concentrations, these values correspond to a $[Cl^-]_i$ of 11.5 [9.8, 11.8] mM (n = 7) and 14.8 [9.4, 20.3] mM (n = 58), respectively (Fig. 1C). These $[Cl^-]_i$ values were also not significantly different ($p = 0.117$, Mann–Whitney).

In order to determine the kinetics of passive Cl^--efflux and to confirm that this high $[Cl^-]_i$ was maintained by the activity of the NKCC1[14,35], we first analyzed the effect of the NKCC1 inhibitor bumetanide on $[Cl^-]_i$. Bath application of 10 µM bumetanide resulted in a significant ($p = 0.028$, Wilcoxon) decline of $[Cl^-]_i$ from 14.5 [11.5, 21.6] mM (n = 6) to 10.2 [9.0, 11.8] mM (n = 6) within ~ 10 min (Fig. 1D,E). This decline in the $[Cl^-]_i$ could be fitted by a monoexponential function using a τ of 381 s (Fig. 1D). From this function we estimated a maximal passive Cl^- efflux of 15.5 µM/s at a $[Cl^-]_i$ of ~ 15 mM. The $[Cl^-]_i$ of 10.2 [9.0, 11.8] mM (n = 6) obtained in the presence of bumetanide is in the range of the passive Cl^- distribution of 9.1 mM. In summary, this result confirms that NKCC1 substantially contribute to the active Cl^- accumulation and is counteracting a passive Cl^- efflux[5,8].

Estimation of the capacity of NKCC1 mediated Cl^- uptake. Since the kinetics of $[Cl^-]$ transport is one major factor influencing ionic plasticity[17,26–28,39,40], we next determined the kinetic properties of Cl^- uptake after an artificial $[Cl^-]_i$ reduction. To quantify the kinetics of the $[Cl^-]_i$ reuptake we decreased $[Cl^-]_i$ by 25 pulses of either 1–3 mM glycine or 30 µM muscimol applied with a frequency of 0.5 Hz to voltage-clamped neurons (Fig. 2A). This procedure significantly ($p = 0.002$, Wilcoxon) reduced the $[Cl^-]_i$ by 3.2 [2.6, 3.8] mM (n = 12) from 11.4 [10.3, 11.8] mM to 7.9 [7.7, 8.4] mM (Fig. 2B). As neither the amount of the $[Cl^-]_i$ decrease ($p = 0.808$, Mann–Whitney) nor the time constants of $[Cl^-]_i$ recovery ($p = 0.291$, Mann–Whitney) were significantly different between glycine- and muscimol-application experiments, the data was pooled. The subsequent recovery of $[Cl^-]_i$ was monitored by determining E_{REV} with a small number of test pulses given at intervals of ~ 100 s, to avoid substantial Cl^- fluxes by these test pulses[4]. These experiments showed that $[Cl^-]_i$ returned to the resting values within ~ 10 min (Fig. 2C). This increase in $[Cl^-]_i$ could be described with a monoexponential function using a time constant τ of 155 s. At a $[Cl^-]_i$ of 9.1 mM, which represents a passive distribution at − 70 mV holding potential and thus eliminates passive fluxes, the active Cl^- uptake rate amounted to 15.4 µM/s. In summary, these results indicate that NKCC1-mediated Cl^- uptake is sufficient to maintain $[Cl^-]_i$ at the observed values, but that this transport process is rather slow in immature CA3 pyramidal neurons.

Effect of spontaneous phasic GABAergic activity. Given the low capacity of NKCC1-mediated Cl^--uptake, we next investigate whether GABAergic activity can override $[Cl^-]_i$ homeostatic processes and thus influence the steady-state $[Cl^-]_i$ levels. In accordance with previous publications that demonstrated substantial $[Cl^-]_i$ changes upon frequent activation of $GABA_A$ receptors[15,16], we observed that the repetitive application of 25

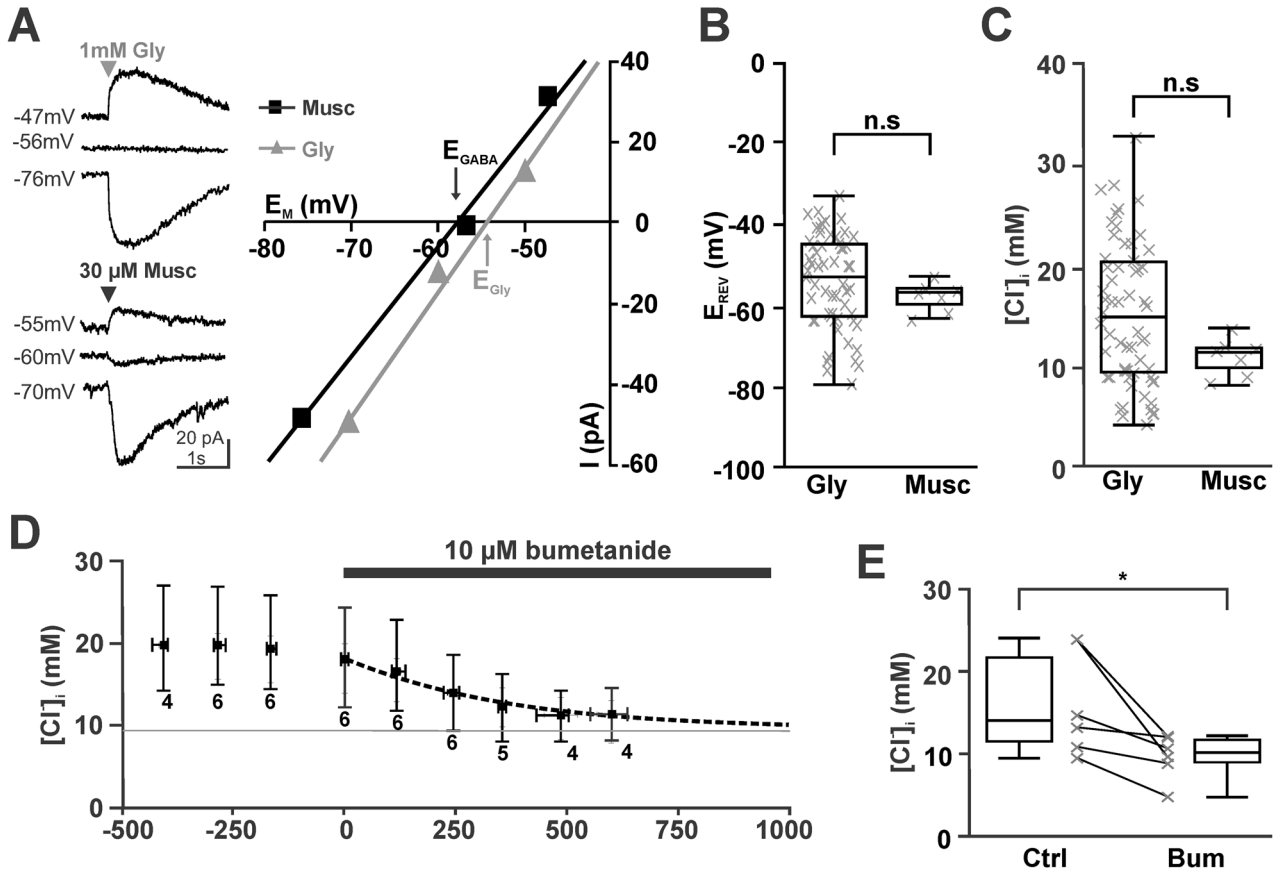

Figure 1. Inhibition of NKCC1 with bumetanide leads to a slow $[Cl^-]_i$ decrease. (**A**) Determination of reversal potentials for GABAergic (black) and glycinergic (gray) currents measured under gramicidin-perforated conditions. The left traces represent typical current traces upon focal application of 1 mM glycine (upper traces) and 30 µM muscimol (lower traces). Only 3 agonist applications at 3 different holding potentials were performed to minimize the effects of agonist–evoked Cl^- currents on $[Cl^-]_i$. (**B**) Box plot diagrams illustrating that glycinergic and GABAergic reversal potentials are comparable. (C) The $[Cl^-]_i$ calculated from the reversal potentials revealed comparable values for both agonists. (**D**) Bath application of 10 µM bumetanide induced an exponential decrease of $[Cl^-]_i$ (dashed line) towards the passive distribution (gray line). Data points represent median ± interquartile range, number of experiments are indicated below the error bars. E: Statistical analysis demonstrating the reliable decrease of $[Cl^-]_i$ in all experiments.

muscimol (30 µM) pulses with a frequency of 0.5 Hz led to a significant ($p = 0.003$, Wilcoxon) decrease in $[Cl^-]_i$ by 3.1 [2.2, 3.7] mM (n = 11) (Fig. 2D,E).

Since this result indicates that GABAergic activity has the potential to contribute to $[Cl^-]_i$ homeostasis, we next investigated whether the observed levels of spontaneous synaptic (phasic) GABAergic activity or the tonic GABAergic conductance influence the resting $[Cl^-]_i$ of pyramidal cells. For this purpose, GABAergic current are isolated by bath application of the glutamatergic antagonists CNQX (30 µM) and APV (20 µM). In line with previous studies reporting a moderate frequency of $GABA_A$ mediated synaptic events in the immature hippocampus[13,41,42], the frequency of pharmacologically isolated GABAergic PSCs in the present study was 2.03 [1.28, 2.03] Hz (n = 6 cells with 1531 events), with a median amplitude of 8.5 [7.3, 14.8] pA (corresponding to a peak conductance of 122 [105.4, 213.6] pS). These GABAergic PSCs were completely suppressed in the presence of 1 µM gabazine (Fig. 3A), which at this concentration selectively blocks synaptic $GABA_A$ receptors[13]. To unravel whether an inhibition of synaptic GABAergic activity influences $[Cl^-]_i$, we determined $[Cl^-]_i$ before and after synaptic GABAergic activity was inhibited for 5—16 min under current clamp conditions. These experiments revealed that after a complete blockade of spontaneous GABAergic inputs, $[Cl^-]_i$ was non-significantly ($p = 0.161$, Wilcoxon test) altered by 0.7 [-0.5, 1.6] mM (n = 8) from 18.3 [15.8, 23.8] mM to 19.2 [17.1, 23.0] mM (Fig. 3B). Note that the tendency ($p = 0.07$, Mann–Whitney U-test) to higher basal $[Cl^-]_i$ in these neurons, as compared to all recordings, led to a higher driving force for Cl^- ions and would thus result in even higher activity-dependent $[Cl^-]_i$ changes. We conclude from these results that the capacity of NKCC1-mediated Cl^- uptake in immature CA3 pyramidal neurons is sufficient to cope with the Cl^--influx caused by spontaneous GABAergic synaptic inputs.

Tonic currents mediated by extrasynaptic GABA receptors contribute substantially to passive $[Cl^-]_i$ fluxes in immature neurons [4], as such tonic currents mediate a larger charge transfer[43]. Since in the immature hippocampus extrasynaptic receptors substantially contribute to the excitability[9,13,41], we also investigated whether tonic GABAergic currents influence $[Cl^-]_i$. For this purpose, we blocked tonic and phasic GABAergic currents

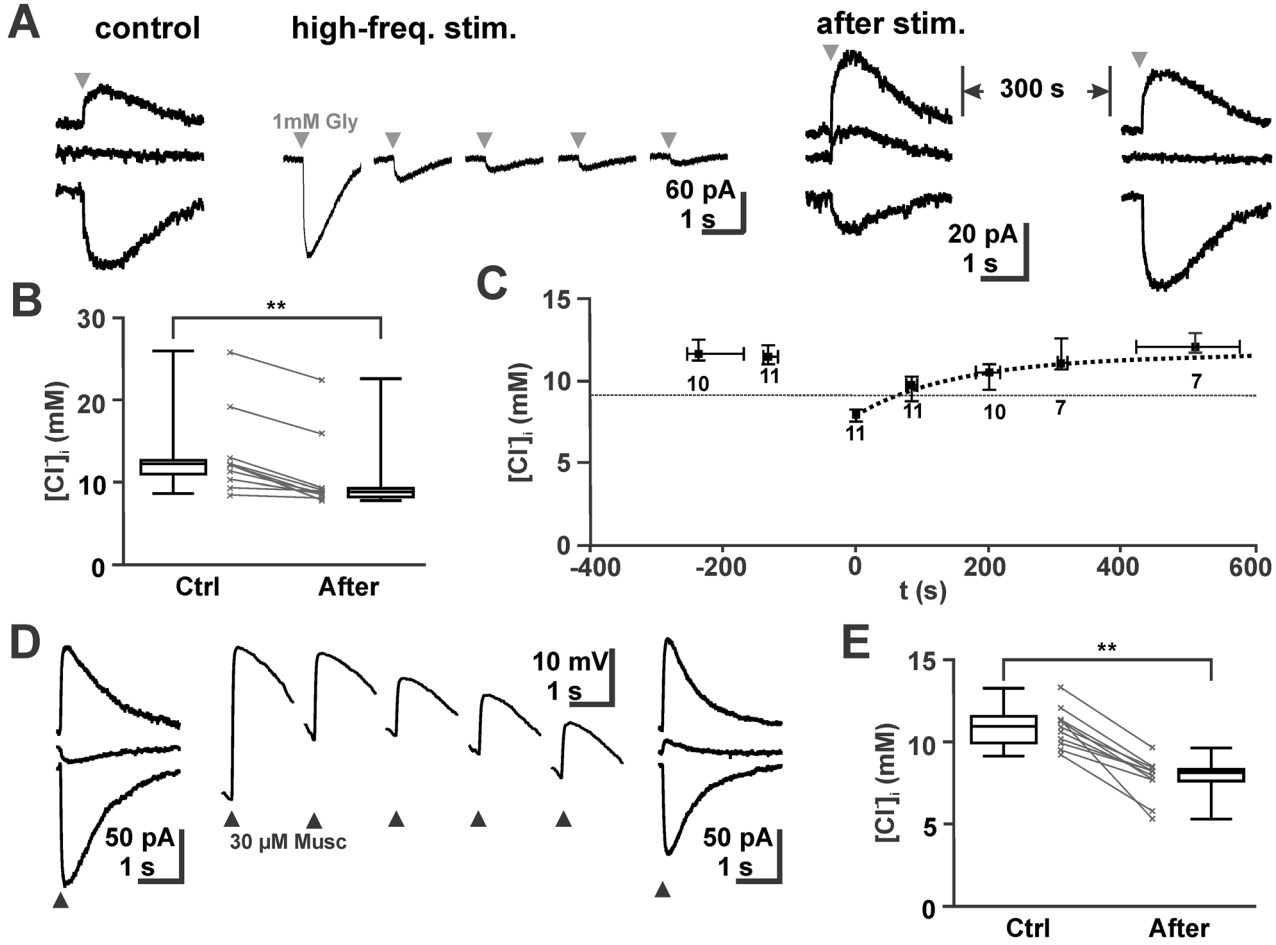

Figure 2. Slow recovery of $[Cl^-]_i$ after depletion. (**A**) Typical current traces upon application of 1 mM glycine at holding potentials of − 43, − 53 and − 73 mV. The thin traces represent representative current traces during the unloading protocol. Note the obvious shift in E_{REV} after the unloading protocol, which reversed after 300 s. (**B**) Statistical analysis demonstrating the reliable decrease of $[Cl^-]_i$ in all experiments upon repetitive stimulation. (**C**) Analysis of $[Cl^-]_i$ before and after the stimulation protocol revealed that $[Cl^-]_i$ recovered with an exponential time course (dashed line) towards the baseline $[Cl^-]_i$. Data points represent median ± interquartiles, number of experiments are indicated below the error bars. (**D**) Typical current traces upon application of 30 µM muscimol. Note the obvious shift in E_{REV} after repetitive muscimol application under current-clamp conditions. (**E**) Analysis of $[Cl^-]_i$ before and after repetitive muscimol application revealed that $[Cl^-]_i$ was significantly reduced after massive GABAergic stimulation.

with picrotoxin[13]. Bath application of 100 µM picrotoxin unravelled a tonic GABAergic conductance of 0.9 [0.49, 1.01] pS (n = 9). The continuous application of 100 µM PTX for 5–12 min led under voltage-clamp conditions to a slight, but significant ($p = 0.008$, Wilcoxon test) increase in $[Cl^-]_i$ by 1.6 [0.7, 1.9] mM (n = 9) from 10.8 [7.3, 11.3] mM to 12.7 [8.1, 13.5] mM (Fig. 3C,D).

In line with this observation, enhancement of tonic conductance using THIP led to a small decrease in $[Cl^-]_i$. To avoid the induction of epileptiform activity by THIP[13], these experiments are performed in the continuous presence of the glutamatergic antagonists CNQX (30 µM) and APV (20 µM). Bath application of 1 µM THIP activated a median membrane conductance of 0.28 [0.03, 0.81] pS (n = 14), which increased to 0.37 [0.09, 1.01] pS (n = 13) and 0.67 [0.02, 1.35] pS (n = 12) in the presences of 3 µM and 10 µM THIP, respectively (Fig. 3E). These enhanced tonic currents led to a significant ($p = 0.033$, Mann–Whitney U-tests) decrease in $[Cl^-]_i$ (Fig. 3F). Upon a constant THIP application for 4 – 12 min $[Cl^-]_i$ decreased in the presence of 3 µM THIP by 3.0 [1.8, 6.9] mM (n = 13, $p = 0.009$, Wilcoxon test) and in 10 µM THIP by 5.0 [0.5, 10.3] mM (n = 12, $p = 0.015$, Wilcoxon test). In the presence of 1 µM THIP no significant ($p = 0.638$, Wilcoxon test) $[Cl^-]_i$ alteration (0.09 [-3.4, 4.4] mM, n = 14) was observed. In summary, these results suggest that basal levels of tonic GABAergic activity can induce Cl^- fluxes that influence mildly the resting $[Cl^-]_i$.

Estimation of activity dependent $[Cl^-]_i$ alterations using compartmental modeling. Finally, we used a data-driven biophysical model of Cl^- dynamics to estimate whether Cl^- fluxes due to synaptic (phasic) and extrasynaptic (tonic) activation of $GABA_A$ channels, transmembrane Cl^- transport and Cl^- diffusion are able to account for the observed stability of $[Cl^-]_i$. To set the geometry of this computational model we employed the

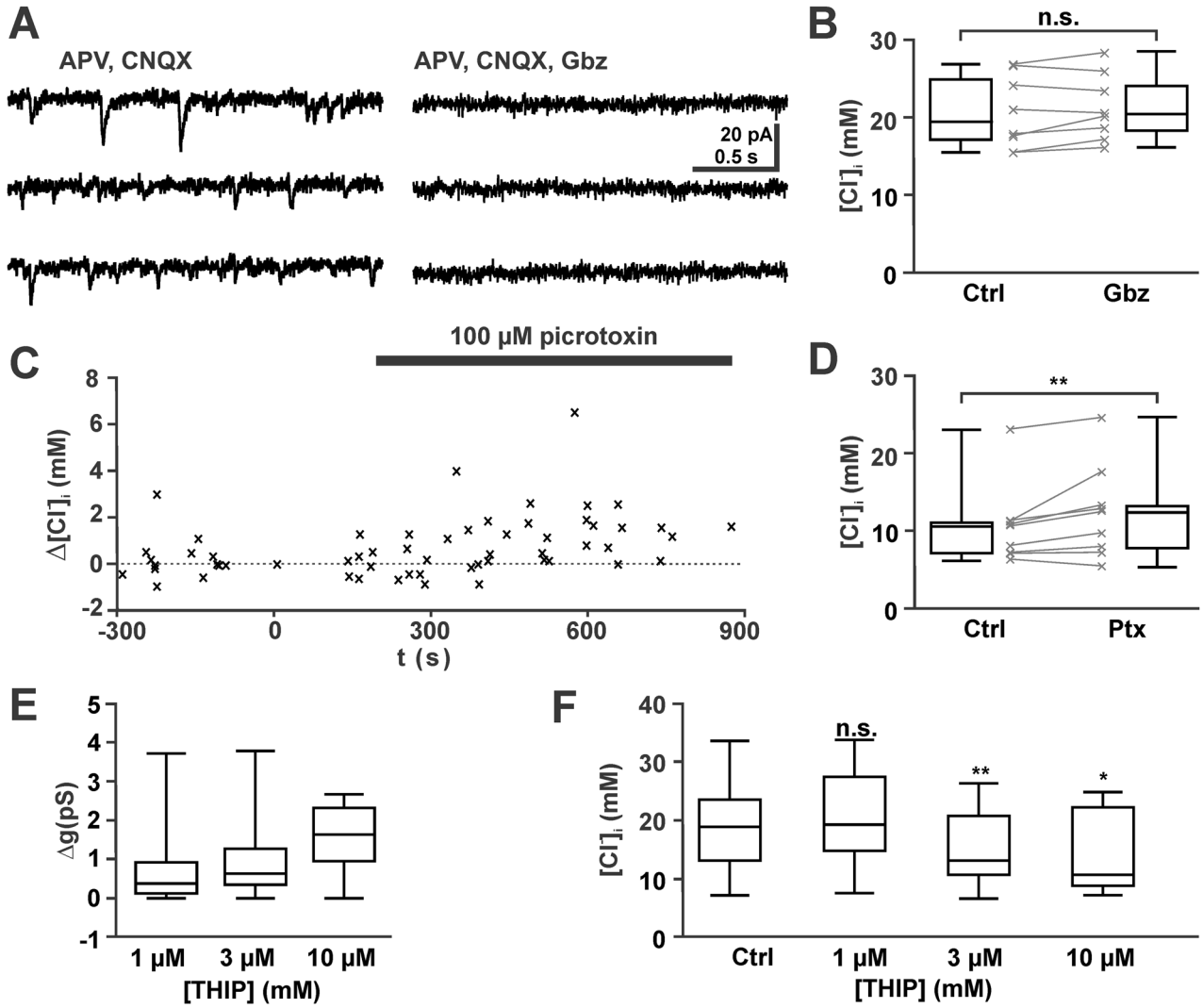

Figure 3. No effect of phasic (synaptic) and mild effect of tonic GABAergic activity on $[Cl^-]_i$. (**A**) Typical current traces illustrating that pharmacologically isolated GABAergic PSCs were completely suppressed by 1 µM gabazine (Gbz). (**B**) Statistical analysis illustrating that a complete suppression of GABAergic PSCs has no significant effect on $[Cl^-]_i$. (**C**) Shift in $[Cl^-]_i$ upon bath application of 100 µM picrotoxin (Ptx) under voltage-clamp conditions. Ptx inhibits both tonic (extrasynaptic) as well as phasic (synaptic) GABAergic currents. Each symbol represents an individual data point from n = 9 experiments. The $[Cl^-]_i$ was related to the $[Cl^-]_i$ in the last measurement before Ptx application. Note the tendency toward an increased $[Cl^-]_i$ in the presence of Ptx. (**D**) Statistical analyses of these experiments revealed an increased $[Cl^-]_i$ after the onset of Ptx application. (**E**) Bath application of THIP dose-dependently increased the membrane conductance. THIP enhances tonic (extrasynaptic) GABAergic conductance. F: Statistical analysis illustrating that THIP induced a dose-dependent decrease in $[Cl^-]_i$.

3D-reconstructed morphology of a young CA3 pyramidal cell (Fig. 4A). The diffusion of Cl^- inside the dendritic tree was simulated using deterministic compartmental diffusion modeling implemented in NEURON[40,44] (see Methods). To simulate tonic GABAergic currents, we added a tonic conductance of 8.75 nS/cm^2, which allowed the model to replicate the passive Cl^- fluxes observed in immature CA3 neurons (Fig. 4B). Next we implemented an active Cl^- accumulation process with a τ_{Cl} of 78.5 s and a target $[Cl^-]_i$ ($[Cl^-]_i^0$) of 13.3 mM, which allowed the modeled neurons to replicate the experimentally determined kinetics of $[Cl^-]_i$ relaxation and the steady-state $[Cl^-]_i$ (Fig. 4C).

To simulate phasic GABAergic activity, we modeled stochastic activation of 107 $GABA_A$ synapses located randomly in the soma and perisomatic dendrites[45] (Fig. 4D). The initial values for the conductance of $GABA_A$ synapses (g_{GABA} = 169 pS) and the frequency of GABAergic synaptic currents (2.14 Hz) were based on the mean values of the experimental data. In accordance with the patch-clamp observation, addition of physiological levels of GABAergic synaptic inputs had only a marginal effect on $[Cl^-]_i$. After 100 s of continuous GABAergic activity at 2.14 Hz $[Cl^-]_i$ decreased by only 0.012 mM (Fig. 4E,F). Augmenting g_{GABA} enhanced the synaptically evoked $[Cl^-]_i$ decline (Fig. 4F), which however remained small (0.114 mM) even if g_{GABA} was increased to 1.69 nS. Increasing the frequency of GABAergic synaptic inputs from 2.14 to 5.35 Hz had only a marginal effect of

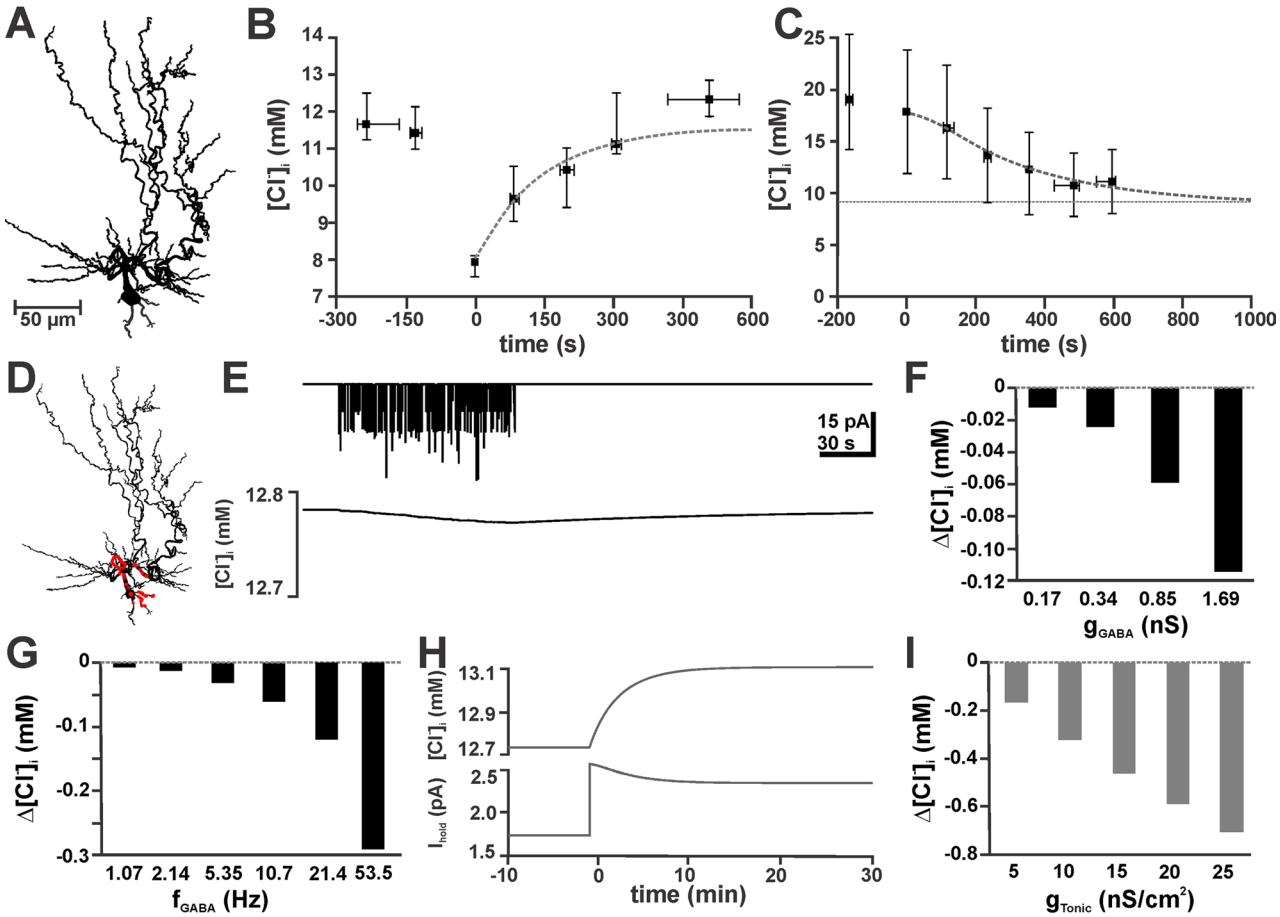

Figure 4. A biophysically realistic compartmental model of active Cl^-uptake and diffusion confirmed limited alterations in $[Cl^-]_i$ due to phasic and tonic GABAergic currents. (**A**) Morphology of the reconstructed CA3 pyramidal cell used for numerical simulations. (**B**) Fit of the experimentally observed $[Cl^-]_i$ relaxation after Cl^- depletion with adequate parameter settings ($\tau = 78.5$ s; $[Cl^-]_i^0 = 13.3$ mM) for a simulated active Cl^- accumulation process (dashed line). (C) Simulation of the experimentally observed $[Cl^-]_i$ decline after elimination of active Cl^- accumulation (black symbols) by implementation of a passive tonic Cl^- conductance at a density of 8.75 nS/cm^2 (dashed line) in a simulated neuron lacking active Cl^--uptake. (**D**) Representation of the reconstructed neuron in the NEURON model. The locations of GABAergic synapses are indicated by red dots. (**E**) Holding current (upper panel) and $[Cl^-]_i$ (lower panel) upon repetitive synaptic stimulation (g_{GABA} 0.169 nS at 2.14 Hz for 100 s). (**F**) $[Cl^-]_i$ changes induced by 100 s of random synaptic activity with different g_{GABA}. (**G**) $[Cl^-]_i$ changes induced by 100 s of random synaptic activity with a g_{GABA} of 0.169 nS at different frequencies. Note that, in line with experiments, physiological values (0.169 nS at 2.14 Hz) induced only marginal $[Cl^-]_i$ changes. (**H**) $[Cl^-]_i$ and holding-current (I_{hold}) upon elimination of the basal tonic GABAergic conductance of 8.75 nS/cm^2 at t = 0. (**I**) $[Cl^-]_i$ changes induced by the addition of a tonic GABAergic component to the basal tonic current.

the $[Cl^-]_i$ change (0.031 mM, Fig. 4G), but at frequencies of ~ 20 and ~ 50 Hz $[Cl^-]_i$ changes by 0.12 mM and 0.29 mM, respectively, were induced (Fig. 4G). In summary, these results indicate that basal levels of synaptic activity had no major effect in $[Cl^-]_i$.

To analyze the influence of tonic GABAergic currents, we omitted the tonic GABAergic conductance of 8.75 nS/cm^2, which changed the holding current (I_{hold}) by 0.8 pA and led to a $[Cl^-]_i$ increase by 0.32 mM (Fig. 4H). Enhancing tonic GABAergic currents by adding multiples of 5 nS/cm^2 to the basal tonic conductance induced a dose-dependent decrease in $[Cl^-]_i$ that, however, remained below 0.8 mM (Fig. 4I). These additional tonic conductances between 5 and 25 nS/cm^2 induced a linear decrease in the inward current between – 0.3 and – 1.28 pA, respectively.

In summary, these simulations with a realistic computational model of Cl^- dynamics support the observation, that NKCC1-mediated Cl^- transport is sufficient to maintain $[Cl^-]_i$ at basal levels of phasic GABAergic activity, while tonic currents have a mild effect on steady-state $[Cl^-]_i$.

Discussion

To comprehend the physiological role of depolarizing GABAergic responses in the immature hippocampus under conditions that dynamically challenge $[Cl^-]_i$ homeostasis, information about the kinetic properties of $[Cl^-]_i$ homeostasis is required[39]. The main findings of the present study can be summarized as follows: (i) NKCC1 is the main Cl^- transporter in immature CA3 pyramidal cells and mediates an active Cl^--accumulation with a rate of 15.4 µM/s. (ii) Physiological levels of tonic GABAergic activation induce a slight decrease in $[Cl^-]_i$ by 1.6 mM. (iii) In contrast, spontaneous phasic GABAergic PSCs do not significantly affect $[Cl^-]_i$. We conclude from these results, that the $[Cl^-]_i$ of immature CA3 pyramidal neurons represents a steady-state equilibrium between active NKCC1-mediated Cl^--accumulation and passive Cl^--efflux, mainly via tonic GABAergic currents. The capacity of the NKCC1-mediated Cl^- uptake in CA3 pyramidal cells is, however, sufficient to maintain a high $[Cl^-]_i$ under basal levels of GABAergic activity.

In the present study we used relative HCO_3^- permeability ratios of 0.18 for $GABA_A$ and of 0.11 for glycine receptors, which were determined by Bormann et al. in cultured spinal cord neurons[38]. While published permeability ratios for $GABA_A$ (0.44) and glycine receptors (0.40) in hippocampal neurons are available[46], using these values resulted in unrealistically low $[Cl^-]_i$ values (ranging from 0.4 to 30 mM). Therefore we prefer to use the values provided by Bormann et al.[38]. Importantly, the qualitative results of our study will not be altered, if the higher relative HCO_3^- permeability ratios are used.

The first outcome of this study is that inhibition of NKCC1 with 10 µM bumetanide induced a decline in $[Cl^-]_i$ towards the passive distribution, which supports the fact that this transporter constitutes the main Cl^- uptake mechanism in immature CA3 pyramidal cells[14,35,47]. Bumetanide has been reported to also inhibit other targets, like KCC2 or aquaporins[48,49], however, at slightly higher effective doses of 55 µM and 100 µM, respectively. An inhibition of these transporters will have no effect on the time constant of the $[Cl^-]_i$ decay upon bumetanide application, but our experiments could not exclude a minor contribution of the $[Cl^-]_i$ extruder KCC2 to steady-state $[Cl^-]_i$ levels. The $[Cl^-]_i$ decline observed in this experiment upon pharmacological inhibition of NKCC1 represents basal Cl^- fluxes, which can be mediated via different types of voltage-, volume-, or ligand-gated Cl^- channels[50]. Next, we determined the capacity of the NKCC1-mediated Cl^--uptake system by quantifying the rate of Cl^--accumulation after $[Cl^-]_i$ depletion. Because the $[Cl^-]_i$ recovery depends only on the properties of the uptake systems and should be independent of the agonists used for the induction of the $[Cl^-]_i$ depletion and since the time constants of $[Cl^-]_i$ recovery are not significantly different between glycine- and muscimol-application, data of muscimol- and glycine application experiments were pooled. In these experiments we determined an uptake rate of 15.4 µM/s. This value was comparable to the $[Cl^-]_i$ uptake rate determined previously in immature cortical neurons[4]. In more mature neurons inhibition of transmembrane Cl^- transport with furosemide induced a positive shift in E_{GABA}, indicating that in slightly older neurons the activity of KCC2 is required to establish a low $[Cl^-]_i$[51].

The maximal rate for passive Cl^- efflux during the $[Cl^-]_i$ decline amounted to ~ 15.5 µM/s and is thus in the range of the Cl^--uptake. However, while the effective rate of Cl^--uptake was determined at 9.1 mM, which is the passive $[Cl^-]_i$-distribution and thus omits any passive Cl^--fluxes, the rate of Cl^--efflux was determined at an arbitrary $[Cl^-]_i$ value of 15 mM. Please note, that both fluxes depend on the $[Cl^-]_i$-gradient across the membrane, with the passive fluxes disappearing at 9.1 mM, while the NKCC1-mediated uptake has a considerably lesser dependency of the $[Cl^-]_i$ gradient[5]. Thus the combination of these oppositely directed Cl-fluxes resulted in a steady-state equilibrium[39], which is maintained at a $[Cl^-]_i$ substantially higher than the passive distribution and thus supports depolarizing GABAergic responses. On the other hand, one should keep in mind that the present study only revealed the properties of the $[Cl^-]_i$ homeostasis in the soma. Variation in the functional expression of active Cl^--transport and passive Cl^--fluxes may result in different capacities of $[Cl^-]_i$ homeostasis in distinct compartments.

Further experiments of the present study revealed, that inhibition of phasic, synaptic GABAergic inputs did not affect $[Cl^-]_i$. In agreement with this lack of an effect of phasic GABAergic inputs on $[Cl^-]_i$, the compartmental simulations in NEURON revealed no major shifts in $[Cl^-]_i$ upon realistic background activation of synaptic GABAergic inputs. In addition, the simulations demonstrated that moderate enhancement of either frequency or conductance of GABAergic synaptic inputs induced only small changes in $[Cl^-]_i$. Only at frequencies > 10 Hz substantial $[Cl^-]_i$ changes were induced. This observation is in contrast to Cajal-Retzius cells, where already moderate, physiological levels of synaptic GABAergic activity (3.6 ± 0.6 Hz) mediate substantial $[Cl^-]_i$ alterations[19], and to neurons from juvenile hippocampal slice cultures, where ongoing phasic activity is required to allow dynamic changes in E_{GABA}[51]. However, in the present simulations $[Cl^-]_i$ was determined in the soma, to match the modelling results with the experimental design of the gramicidin perforated patch experiments. Within the dendritic compartment these levels of GABAergic synaptic activity will induce substantial GABAergic $[Cl^-]_i$ transients[17].

In addition, the present study demonstrated that inhibition of both, phasic and tonic GABAergic currents with picrotoxin[13] evoked a small, but significant $[Cl^-]_i$ increase. In line with this observation, the pharmacological induction of extrasynaptic GABAergic currents with THIP led to a substantial reduction in $[Cl^-]_i$. This observation could be replicated in the NEURON simulations by the addition of tonic Cl^- conductances. Our experiments suggest that the substantial tonic current found in immature hippocampal neurons[52], contributes to steady state $[Cl^-]_i$. The dissimilar effects of phasic and tonic GABAergic currents directly reflect the different levels of charge transfer mediated by the short phasic responses (ca. 0.015 pC/s at 2.13 Hz and a g_{GABA} of 169 pS) in contrast to the persistent but small amplitude tonic GABAergic currents (ca. 0.46 pC/s at 8.75 nS/cm²)[43].

A variety of studies in the adult brain have shown that excessive GABAergic stimulation can induce Cl^--fluxes that exceed the capacity of active Cl^- transport and consequently increase $[Cl^-]_i$ and alter GABAergic responses[15,16,18,25,40,51,53]. The low capacity of the NKCC1-mediated Cl^- uptake makes immature neurons particularly susceptible to such effects. On the other hand, spontaneous, highly correlated activity transients are typical

for developing neuronal systems[54]. These correlated activity transients are characterized by the synchronous activation of glutamatergic and GABAergic activity[55,56]. The resulting massive GABAergic inputs may exceed the capacity of transmembrane Cl^- transport and induce substantial $[Cl^-]_i$ changes. The depolarizing glutamatergic inputs during correlated network activity can even augment the GABAergic Cl^- fluxes and thus aggravate the $[Cl^-]_i$ alterations[57]. Indeed it has been demonstrated that such physiological bursts of activity can led to substantial $[Cl^-]_i$ shifts in the spinal cord[33,58], neocortex[19], and immature hippocampus[17]. Whereas in the adult system such changes will decrease GABAergic inhibition and thus contribute to the establishment of hyperexcitable states and reduced pharmacological responsiveness[18], in immature neurons the activity-dependent $[Cl^-]_i$ reduction will decrease the excitatory potential of $GABA_A$ receptor-mediated responses. And since shunting inhibition remains constant[55,59], this activity-dependent $[Cl^-]_i$ decrease will augment the inhibitory potential of GABAergic responses. Therefore, the low capacity of Cl^- export in immature neurons may be an adaptation to prevent hyper-excitability mediated by depolarizing GABA responses, as has been originally suggested by Ben-Ari[3]. In addition, at least for the immature spinal cord it has been demonstrated that such activity-dependent $[Cl^-]_i$ transients can determine the frequency of spontaneous activity transients by temporarily reducing the excitatory effect of GABA[58]. Thus it is tempting to speculate that recurrent alterations in $[Cl^-]_i$ may also contribute to slow oscillatory phenomena in other regions of the developing nervous system.

In summary, the results of our present study demonstrate that the capacity of Cl^- accumulation is limited in immature hippocampal CA3 pyramidal neurons. This finding, in combination with a quantification in immature cortical neurons[4] and the observation of activity-related $[Cl^-]_i$ transients in other immature tissues[19,33], suggests that an unstable $[Cl^-]_i$ homeostasis may be an innate feature of immature neurons.

Methods

Slice preparation. All experiments were conducted in accordance with EU directive 86/609/EEC for the use of animals in research and the NIH Guide for the Care and Use of Laboratory Animals, and were approved by the local ethical committee (Landesuntersuchungsanstalt RLP, Koblenz, Germany). All efforts were made to minimize the number of animals and their suffering. Wistar rat pups of P4-7 were obtained from the local breeding facility and were deeply anesthetized with enflurane (Ethrane, Abbot Laboratories, Wiesbaden, Germany). After decapitation, the brains were quickly removed and immersed for 2–3 min in ice-cold standard artificial cerebrospinal fluid (ACSF, composition see below). Coronal slices (400 µm thickness) including the hippocampus were cut on a vibratome (HR2, Sigmann Elektronik, Hüffenhardt, Germany). The slices were stored in an incubation chamber filled with oxygenated ACSF at room temperature before they were transferred to the recording chamber.

Data acquisition and analysis. Gramicidin-perforated whole-cell patch-clamp recordings were performed as described previously[4,13] at 31 ± 1 °C in a submerged-type recording chamber attached to the fixed stage of a microscope (BX51 WI, Olympus). Pyramidal neurons in stratum pyramidale of the CA3 region were identified by their location and morphological appearance in infrared differential interference contrast image. Patch-pipettes (5–12 MΩ) were pulled from borosilicate glass capillaries (2.0 mm outside, 1.16 mm inside diameter, Science Products, Hofheim, Germany) on a vertical puller (PP-830, Narishige) and filled with pipette solution containing 130 KCl, 1 $CaCl_2$, 2 $MgCl_2$, 11 EGTA, 10 HEPES, 2 Na2-ATP, 0.5 Na-GTP (pH adjusted to 7.4 with KOH and osmolarity to 306 mOsm with sucrose). For gramicidin-perforated patch-clamp recordings 10–50 µg/ml gramicidin D (Sigma, St Louis, MO, USA) was added from a stock solution (1–2 mg/ml in DMSO) on the day of experiment. Experiments were omitted from analysis, when an instantaneous or constant shift in the muscimol/glycine reversal potential towards positive values, determined by the high $[Cl^-]$ of the pipette solution, occurred, as they indicate insufficient perforated-patch conditions.

Signals were recorded with a discontinuous voltage-clamp/current-clamp amplifier (SEC05L, NPI, Tamm, Germany), low-pass filtered at 3 kHz and stored and analyzed using an ITC-1600 AD/DA board (HEKA) and TIDA software. Input resistance and capacitance were determined from a series of hyperpolarizing current steps. The apparent cell surface was estimated using a specific capacitance of 2 µF/cm^2. Spontaneous postsynaptic currents (sPSCs) were detected and analysed from whole-cell patch-clamp recordings according to their amplitude and shape by appropriate settings using Minianalysis Software (Synaptosoft, Fort Lee, NJ).

The $[Cl^-]_i$ was determined from the reversal potentials of GABAergic and glycinergic currents recorded under voltage-clamp conditions using the Goldman–Hodgkin–Katz equation:

$$E_{GABA} = \frac{RT}{ZF} * \ln\left(\frac{P_{Cl}\left[Cl^-\right]_e + P_{HCO3}\left[HCO_3^-\right]_e}{P_{Cl}[Cl^-]_i + P_{HCO3}\left[HCO_3^-\right]_i}\right)$$

For the calculation of $[Cl^-]_i$ from E_{GABA} we used a $[Cl^-]_e$ of 133.5 mM, an extracellular HCO_3^- concentration ($[HCO_3^-]_e$) of 24 mM, a $[HCO_3^-]_i$ of 14.1 mM, and published values for the HCO_3^- permeability of GABA (0.18) or glycine (0.11) receptors[38]. GABAergic and glycinergic currents were evoked by brief (2–10 ms) pulses of 30 µM muscimol or 0.2–1 mM glycine from a patch pipette positioned close to the soma via a custom built pressure application system (Lee, Westbrook, CT) at a pressure of 0.5 bar. The use of glycine pulses was necessary to allow the determination of $[Cl^-]_i$ in the presence of gabazine or picrotoxin, which eliminate GABAergic currents[13].

All values were given as median ± interquartile range, in the panels median ± interquartile range was used for time-dependent plots, while summarized results were shown as box and whisker plots (minimum, first quartile, median, third quartile, maximum). For statistical analysis of unpaired data Mann–Whitney U-tests and for paired data Wilcoxon signed-rank test were used (Systat 11, Point Richmond, CA). Significance was assigned at levels of 0.05 (*), 0.01 (**) and 0.001 (***).

Morphological reconstruction. For morphological reconstruction, 18 CA3 pyramidal cells were filled with biocytin under whole-cell conditions. From this 18 stained neurons, two typical cells were used for quantitative somatodendritic reconstruction after visual inspection. For this purpose, 0.5–1% biocytin (Sigma, Taufkirchen, Germany) was added to the pipette solution. After filling of the cells, slices were fixed for at least 24 h in 4% paraformaldehyde. Subsequently they were rinsed and incubated 60 min with 0.5% H_2O_2 and 0.8% Triton-X100 to inhibit endogenous peroxidases. After overnight incubation with an avidin-coupled peroxidase (ABC kit, Vectorlabs, Burlingame, CA, USA), slices were pre-incubated in 0.5 mM diaminobenzidine and subsequently developed in diaminobenzidine and 0.015% H_2O_2. The slices were finally rinsed, dehydrated slowly through alcohol and propylenoxide, and embedded in Durcupan (Fluka, Buchs, Switzerland). Reconstruction and morphological analysis of the biocytin-labelled neurons were performed using the 60 × oil-immersion objective (NA 1.4) of a Nikon Eclipse 80i (Nikon, Germany) attached to a computer system (Neurolucida; MBF Bioscience Europe). Data was corrected for tissue shrinkage after importing to the NEURON environment. For this purpose we used the values suggested by Staiger et al.[60] and expanded the x-/y-dimensions by 12.5% and the z-dimension by 50%.

Compartmental modeling. The reconstructed CA3 pyramidal cell (see above) was imported into the NEURON simulation program (neuron.yale.edu). The following passive parameters were used: R_a (specific axial resistance) = 35.4 Ωcm; g_{pas} (passive specific membrane conductance) = 17.05 nS/cm^2; E_{pas} = -74.05 mV, C_m (specific membrane capacitance) = 1 µF/cm^2. In addition, a tonic leak Cl^- conductance:

$$I_{tonic} = (1-P_{GABA}) \cdot g_{tonic} \cdot (V-E_{Cl}) + P_{GABA} \cdot g_{tonic} \cdot (V-E_{HCO3}).$$

with a conductance g_{tonic} of 8.75 nS/cm^2 was inserted. Implementing these parameters in the reconstructed morphology resulted in a resting membrane potential of − 70 mV and an input resistance of 306 MΩ.

Cl^- diffusion and uptake were calculated by standard compartmental diffusion modeling[40,44]. To simulate intracellular Cl^- dynamics, we adapted our previously published model[40]. Longitudinal Cl^- diffusion along dendrites was modeled as the exchange of Cl^- between adjacent compartments. For radial diffusion, the volume was discretized into a series of 4 concentric shells around a cylindrical core and Cl^- was allowed to flow between adjacent shells[61]. The free diffusion coefficient of Cl^- inside neurons (D_{Cl}) was set to 2 µm^2/ms[53]. To simulate Cl^- uptake, a pump mechanism for transmembrane Cl^- transport was included. Cl^-transport was modeled as exponential recovery of $[Cl^-]_i$ to its target $[Cl^-]_i$ ($[Cl^-]_i^0$) with a time constant τ_{Cl}.

$$\frac{d[Cl^-]_i}{dt} = \frac{[Cl^-]_i^0 - e[Cl^-]_i}{\tau_{Cl}}$$

The pump mechanism approximates an NKCC1-like Cl^- transport mechanism.

The impact of GABAergic Cl^- currents on $[Cl^-]_i$ was calculated as:

$$\frac{d[Cl^-]_i}{dt} = \frac{1}{F}\frac{I_{Cl}}{volume}$$

with F = 96,485 C/mol (Faraday constant). $GABA_A$ synapses were simulated as a postsynaptic parallel Cl^- and HCO_3^- conductance with exponential rise and exponential decay[40]:

$$I_{GABA} = I_{Cl} + I_{HCO3} = (1-P) \cdot g_{GABA} \cdot (V-E_{Cl}) + P \cdot g_{GABA} \cdot (V-E_{HCO3})$$

where P is a fractional ionic conductance that was used to split the $GABA_A$ conductance (g_{GABA}) into Cl^- and HCO_3^- conductance. E_{Cl} and E_{HCO3} were calculated from Nernst equation. The $GABA_A$ conductance was modeled using a two-term exponential function, using values of rise time (0.5 ms) and decay time (37 ms)[17]. Parameters used in our simulations were as follows: $[Cl^-]_o$ = 133.5 mM, $[HCO3^-]_i$ = 14.1 mM, $[HCO3^-]_o$ = 24 mM, temperature = 31 °C, P_{GABA} = 0.18, and P_{Gly} = 0.11[38]. The $GABA_A$ inputs (107 synapses, peak conductance 0.169 nS)[17] were activated stochastically (Poisson) with a frequency of 0.02 Hz, corresponding to a main PSC frequency of 2.14, except where noted. Source codes of all models are available at ModelDB (https://modeldb.yale.edu/266811; password is "hippocampus").

Solutions and drugs. The bathing solution consisted of 126 NaCl, 26 $NaHCO_3$, 1.25 NaH_2PO_5, 1 $MgCl_2$, 2 $CaCl_2$, 2.5 KCl, 10 glucose (pH 7.4, osmolarity 306 mOsm) and was equilibrated with 95% O_2 / 5% CO_2 at least 1 h before use. GABA (γ-amino butyric acid), 6-Imino-3-(4-methoxyphenyl)-1(6H)-pyridazinebutanoic acid hydrobromide (gabazine, SR-95531), picrotoxin (PTX), 4,5,6,7-tetrahydroisoxazolo[5,4-c]-pyridin-3-ol (THIP), glycine and bumetanide were purchased from Sigma, and DL-2-Amino-5-phosphonopentanoic acid (APV), 6-Cyano-7-nitroquinoxaline-2,3-dione (CNQX), muscimol and tetrodotoxin (TTX), from Biotrend (Cologne, Germany). TTX and glycine were dissolved in distilled water and picrotoxin, gabazine, muscimol, bumetanide, CNQX and APV in dimethylsulfoxide (DMSO). All substances were added to the solutions shortly before the experiment. The DMSO concentration of the final solution never exceeded 0.2%.

Received: 29 July 2020; Accepted: 9 October 2020
Published online: 27 October 2020

References

1. Farrant, M. & Kaila, K. The cellular, molecular and ionic basis of GABA(A) receptor signalling. *Prog. Brain Res.* **160**, 59–87 (2007).

2. Swanson, O. K. & Maffei, A. From hiring to firing: activation of inhibitory neurons and their recruitment in behavior. *Front. Mol. Neurosci.* **12**, 1–9 (2019).
3. Ben-Ari, Y. Excitatory actions of GABA during development: the nature of the nurture. *Nat. Rev. Neurosci.* **3**, 728–739 (2002).
4. Achilles, K. *et al.* Kinetic properties of Cl– uptake mediated by Na+-dependent K+-2Cl– cotransport in immature rat neocortical neurons. *J. Neurosci.* **27**, 8616–8627 (2007).
5. Blaesse, P., Airaksinen, M. S., Rivera, C. & Kaila, K. Cation-chloride cotransporters and neuronal function. *Neuron* **61**, 820–838 (2009).
6. Payne, J. A., Rivera, C., Voipio, J. & Kaila, K. Cation-chloride co-transporters in neuronal communication, development and trauma. *Trends Neurosci.* **26**, 199–206 (2003).
7. Gonzalez-Islas, C., Chub, N. & Wenner, P. NKCC1 and AE3 appear to accumulate chloride in embryonic motoneurons. *J. Neurophysiol.* **101**, 507–518 (2009).
8. Watanabe, M. & Fukuda, A. Development and regulation of chloride homeostasis in the central nervous system. *Front. Cell. Neurosci.* **9**, 1–14 (2015).
9. Sipila, S. T., Huttu, K., Soltesz, I., Voipio, J. & Kaila, K. Depolarizing GABA acts on intrinsically bursting pyramidal neurons to drive giant depolarizing potentials in the immature hippocampus. *J. Neurosci.* **25**, 5280–5289 (2005).
10. Kirischuk, S. *et al.* Modulation of neocortical development by early neuronal activity: Physiology and pathophysiology. *Front. Cell. Neurosci.* **11**, 1–21 (2017).
11. Dzhala, V. I., Brumback, A. C. & Staley, K. J. Bumetanide enhances phenobarbital efficacy in a neonatal seizure model. *Ann. Neurol.* **63**, 222–235 (2008).
12. Mazarati, A., Shin, D. & Sankar, R. Bumetanide inhibits rapid kindling in neonatal rats. *Epilepsia* **50**, 2117–2122 (2009).
13. Kolbaev, S. N., Sharopov, S., Dierkes, P. W., Luhmann, H. J. & Kilb, W. Phasic GABAA-receptor activation is required to suppress epileptiform activity in the CA3 region of the immature rat hippocampus. *Epilepsia* **53**, 888–896 (2012).
14. Dzhala, V. I. *et al.* NKCC1 transporter facilitates seizures in the developing brain. *Nat. Med.* **11**, 1205–1213 (2005).
15. Thompson, S. M. & Gahwiler, B. H. Activity-dependent disinhibition. I. Repetitive stimulation reduces IPSP driving force and conductance in the hippocampus in vitro. *J. Neurophysiol.* **61**, 501–511 (1989).
16. Isomura, Y. *et al.* Synaptically activated Cl^- accumulation responsible for depolarizing GABAergic responses in mature hippocampal neurons. *J. Neurophysiol.* **90**, 2752–2756 (2003).
17. Lombardi, A., Jedlicka, P., Luhmann, H. J. & Kilb, W. Giant depolarizing potentials trigger transient changes in the intracellular Cl^- concentration in CA3 pyramidal neurons of the immature mouse hippocampus. *Front. Cell. Neurosci.* **12**, 420 (2018).
18. Lillis, K. P., Kramer, M. A., Mertz, J., Staley, K. J. & White, J. A. Neurobiology of disease pyramidal cells accumulate chloride at seizure onset. *Neurobiol. Dis.* **47**, 358–366 (2012).
19. Kolbaev, S. N., Luhmann, H. J. & Kilb, W. Activity-dependent scaling of GABAergic excitation by dynamic Cl^- changes in Cajal–Retzius cells. *Pflugers Arch. Eur. J. Physiol.* **461**, 557–565 (2011).
20. Raimondo, J. V., Markram, H. & Akerman, C. J. Short-term ionic plasticity at GABAergic synapses. *Front. Synaptic Neurosci.* **4**, 5 (2012).
21. Kaila, K., Ruusuvuori, E., Seja, P., Voipio, J. & Puskarjov, M. GABA actions and ionic plasticity in epilepsy. *Curr. Opin. Neurobiol.* **26**, 34–41 (2014).
22. Wright, R., Raimondo, J. V. & Akerman, C. J. Spatial and temporal dynamics in the ionic driving force for GABA(A) Receptors. *Neural Plast.* **2011**, 728395 (2011).
23. Currin, C. B., Trevelyan, A. J., Akerman, C. J. & Raimondo, J. V. Chloride dynamics alter the input-output properties of neurons. *PLoS Comput. Biol.* **16**, 1–22 (2020).
24. Chub, N., Mentis, G. Z. & O'Donovan, M. J. Chloride-sensitive MEQ fluorescence in chick embryo motoneurons following manipulations of chloride and during spontaneous network activity. *J. Neurophysiol.* **95**, 323–330 (2006).
25. Staley, K. J. & Proctor, W. R. Modulation of mammalian dendritic GABA(A) receptor function by the kinetics of Cl^- and $HCO3^-$ transport. *J. Physiol.* **519**, 693–712 (1999).
26. Lombardi, A., Jedlicka, P., Luhmann, H. J. & Kilb, W. Interactions between membrane resistance, GABA-A receptor properties, bicarbonate dynamics and Cl−-transport shape activity-dependent changes of intracellular Cl– concentration. *Int. J. Mol. Sci.* **20**, 1–22 (2019).
27. Doyon, N. *et al.* Efficacy of synaptic inhibition depends on multiple, dynamically interacting mechanisms implicated in chloride homeostasis. *Plos Comput. Biol.* **7**, e1002149 (2011).
28. Mohapatra, N. *et al.* Spines slow down dendritic chloride diffusion and affect short-term ionic plasticity of GABAergic inhibition. *Sci. Rep.* **6**, 23196 (2016).
29. Doyon, N., Prescott, S. A. & Koninck, Y. D. Mild KCC2 Hypofunction causes inconspicuous chloride dysregulation that degrades neural coding. *Front. Cell. Neurosci.* **9**, 1–16 (201).
30. Buchin, A., Chizhov, A., Huberfeld, G., Miles, R. & Gutkin, B. S. Reduced efficacy of the KCC2 cotransporter promotes epileptic oscillations in a subiculum network model. *J. Neurosci.* **36**, 11619–11633 (2016).
31. Düsterwald, K. M. *et al.* Biophysical models reveal the relative importance of transporter proteins and impermeant anions in chloride homeostasis. *Elife* **7**, 1–30 (2018).
32. Schmidt, T. *et al.* Differential regulation of chloride homeostasis and GABAergic transmission in the thalamus. *Sci. Rep.* **8**, 13929 (2018).
33. Gonzalez-Islas, C., Chub, N., Garcia-Bereguiain, M. A. & Wenner, P. GABAergic synaptic scaling in embryonic motoneurons is mediated by a shift in the chloride reversal potential. *J. Neurosci.* **30**, 13016–13020 (2010).
34. Griguoli, M. & Cherubini, E. Early correlated network activity in the hippocampus: its putative role in shaping neuronal circuits. *Front. Cell. Neurosci.* **11**, 255 (2017).
35. Sipila, S. T., Schuchmann, S., Voipio, J., Yamada, J. & Kaila, K. The cation-chloride cotransporter NKCC1 promotes sharp waves in the neonatal rat hippocampus. *J. Physiol.* **573**, 765–773 (2006).
36. Chen, R. *et al.* Activation of glycine receptors modulates spontaneous epileptiform activity in the immature rat hippocampus. *J. Physiol.* **592**, 2153–2168 (2014).
37. Xiong, G., Metheny, H., Johnson, B. N. & Cohen, A. S. A comparison of different slicing planes in preservation of major hippocampal pathway fibers in the mouse. *Front. Neuroanat.* **11**, 1–17 (2017).
38. Bormann, J., Hamill, O. P. & Sakmann, B. Mechanism of anion permeation through channels gated by glycine and gamma-aminobutyric acid in mouse cultured spinal neurones. *J. Physiol.* **385**, 243–286 (1987).
39. Doyon, N., Vinay, L., Prescott, S. A. & De Koninck, Y. Chloride regulation: a dynamic equilibrium crucial for synaptic inhibition. *Neuron* **89**, 1157–1172 (2016).
40. Jedlicka, P., Deller, T., Gutkin, B. S. & Backus, K. H. Activity-dependent intracellular chloride accumulation and diffusion controls GABAA receptor-mediated synaptic transmission. *Hippocampus* **21**, 885–898 (2011).
41. Marchionni, I., Omrani, A. & Cherubini, E. In the developing rat hippocampus a tonic GABA A—mediated conductance selectively enhances the glutamatergic drive of principal cells. *J. Physiol.* **581**, 515–528 (2007).
42. Tyzio, R., Holmes, G. L., Ben-Ari, Y. & Khazipov, R. Timing of the developmental switch in GABAA mediated signaling from excitation to inhibition in CA3 rat hippocampus using gramicidin perforated patch and extracellular recordings. *Epilepsia* **48**, 96–105 (2007).

43. Mody, I. & Pearce, R. A. Diversity of inhibitory neurotransmission through GABA(A) receptors. *Trends Neurosci.* **27**, 569–575 (2004).
44. Mohapatra, N., Santamaria, F. & Jedlicka, P. Modeling the effects of neuronal morphology on dendritic chloride diffusion and GABAergic inhibition. *BMC Neurosci.* **6**, 23196 (2014).
45. Papp, E., Leinekugel, X., Henze, D. A., Lee, J. & Buzsáki, G. The apical shaft of CA1 pyramidal cells is under GABAergic interneuronal control. *Neuroscience* **102**, 715–721 (2001).
46. Fatima-Shad, K. & Barry, P. H. Anion permeation in GABA- and glycine-gated channels of mammalian cultured hippocampal neurons. *Proc. R. Soc. B Biol. Sci.* **253**, 69–75 (1993).
47. Sipilä, S. T. *et al.* Compensatory enhancement of intrinsic spiking upon NKCC1 disruption in neonatal hippocampus. *J. Neurosci.* **29**, 6982–6988 (2009).
48. Payne, J. A. Functional characterization of the neuronal-specific K-Cl cotransporter: Implications for [K+](o) regulation. *Am. J. Physiol. Cell Physiol.* **273**, C1516–C1525 (1997).
49. Migliati, E. *et al.* Inhibition of aquaporin-1 and aquaporin-4 water permeability by a derivative of the loop diuretic bumetanide acting at an internal pore-occluding binding site. *Mol. Pharmacol.* **76**, 105–112 (2009).
50. Jentsch, T. J., Pusch, M., Rehfeldt, A. & Steinmeyer, K. The ClC family of voltage-gated chloride channels: structure and function. *Ann. N.Y. Acad. Sci.* **707**, 285–293 (1993).
51. Thompson, S. M. & Gahwiler, B. H. Activity-dependent disinhibition. II. Effects of extracellular potassium, furosemide, and membrane potential on E(Cl)—in hippocampal CA3 neurons. *J. Neurophysiol.* **61**, 512–523 (1989).
52. Sipilä, S. T., Voipio, J. & Kaila, K. GAT-1 acts to limit a tonic GABAA current in rat CA3 pyramidal neurons at birth. *Eur. J. Neurosci.* **25**, 717–722 (2007).
53. Kuner, T. & Augustine, G. J. A genetically encoded ratiometric indicator for chloride: capturing chloride transients in cultured hippocampal neurons. *Neuron* **27**, 447–459 (2000).
54. Luhmann, H. J. *et al.* Spontaneous neuronal activity in developing neocortical networks: From single cells to large-scale interactions. *Front. Neural Circuits* **10**, 40 (2016).
55. Khalilov, I., Minlebaev, M., Mukhtarov, M. & Khazipov, R. Dynamic changes from depolarizing to hyperpolarizing GABAergic actions during giant depolarizing potentials in the neonatal rat hippocampus. *J. Neurosci.* **35**, 12635–12642 (2015).
56. Khazipov, R. *et al.* Early development of neuronal activity in the primate hippocampus in utero. *J. Neurosci.* **21**, 9770–9781 (2001).
57. Halbhuber, L., Achtner, C., Luhmann, H. J., Sinning, A. & Kilb, W. Coincident activation of glutamate receptors enhances GABAA receptor-induced ionic plasticity of the intracellular Cl− concentration in dissociated neuronal cultures. *Front. Cell. Neurosci.* **13**, 1–15 (2019).
58. Chub, N. & O'Donovan, M. J. Post-episode depression of GABAergic transmission in spinal neurons of the chick embryo. *J. Neurophysiol.* **85**, 2166–2176 (2001).
59. Kolbaev, S. N., Achilles, K., Luhmann, H. J. & Kilb, W. Effect of depolarizing $GABA_A$-mediated membrane responses on excitability of cajal-retzius cells in the immature rat neocortex. *J. Neurophysiol.* **106**, 2034–2044 (2011).
60. Staiger, J. F., Bojak, I., Miceli, S. & Schubert, D. A gradual depth-dependent change in connectivity features of supragranular pyramidal cells in rat barrel cortex. *Brain Struct. Funct.* **220**, 1317–1337 (2015).
61. Hines, M. L. & Carnevale, N. T. Expanding NEURON's repertoire of mechanisms with NMODL. *Neural Comput.* **12**, 995–1007 (2000).

Acknowledgements

The authors thank Beate Krumm, for excellent technical assistance. RC was graduate student of the Neuroscience Graduate School at the University of Mainz. AL received a stipend from the FTN and was a graduate student in the TrandsMed program. The work was supported by supported by a BMBF grant to PJ (No. 031L0229) and DFG grants to WK (KI 835/3) and HJL (SFB 1080-A01).

Author contributions

W.K., and P.J. conceptualized the study, S.N.K. and R.C. performed the electrophysiological recordings, J.F.S. provided the neuronal reconstruction, N.M., A.L., P.J. and W.K. programmed and analyzed the in-silico modelling, W.K. and H.J.L. wrote the manuscript. All authors have read and agreed on the final version of the manuscript.

Funding

Open Access funding enabled and organized by Projekt DEAL.

Competing interests

All authors declare that they have no competing financial, professional or personal interests that might have influenced the objectives, performance or presentation of the study described in this manuscript.

Additional information

Correspondence and requests for materials should be addressed to W.K.